



Article

Microbial Markers Profile in Anaerobic Mars Analogue Environments Using the LDChip (Life Detector Chip) Antibody Microarray Core of the SOLID (Signs of Life Detector) Platform

Laura García-Descalzo ^{1,*}, Victorino Parro ¹, Miriam García-Villadangos ¹, Charles S. Cockell ², Christine Moissl-Eichinger ^{3,4}, Alex Perras ^{3,5}, Petra Rettberg ⁶ , Kristina Beblo-Vranesevic ⁶ , Maria Bohmeier ⁶ , Elke Rabbow ⁶, Frances Westall ⁷, Frederik Gaboyer ⁷, Ricardo Amils ^{1,8} , Moustafa Malki ⁸, Viggo Marteinson ^{9,10} , Pauline Vannier ⁹, Pascale Ehrenfreund ¹¹, Euan Monaghan ¹¹, Andreas Riedo ¹¹, Patricia Cabezas ¹², Nicolas Walter ¹² and Felipe Gómez Gómez ¹

¹ Centro de Astrobiología (CSIC-INTA), 28850 Madrid, Spain; parrov@cab.inta-csic.es (V.P.); villadangosgm@cab.inta-csic.es (M.G.-V.); ramils@cbm.uam.es (R.A.); gomezgf@cab.inta-csic.es (F.G.G.)

² UK Center for Astrobiology, School of Physics and Astronomy, University of Edinburgh, Edinburgh EH9 3FD, UK; c.s.cockell@ed.ac.uk

³ Department of Internal Medicine, Medical University of Graz, 8036 Graz, Austria; christine.moissl-eichinger@medunigraz.at (C.M.-E.); akperras@gmail.com (A.P.)

⁴ BioTechMed Graz, 8010 Graz, Austria

⁵ Department of Microbiology and Archaea, University of Regensburg, 93040 Regensburg, Germany

⁶ German Aerospace Center (DLR), Research Group 'Astrobiology', Radiation Biology Department, Institute of Aerospace Medicine, 51147 Cologne, Germany; Petra.Rettberg@dlr.de (P.R.); Kristina.Beblo@dlr.de (K.B.-V.); Maria.Bohmeier@dlr.de (M.B.); Elke.Rabbow@dlr.de (E.R.)

⁷ Centre de Biophysique Moléculaire, Centre National de la Recherche Scientifique (CNRS), 45100 Orléans, France; frances.westall@cnrs-orleans.fr (F.W.); frederic.gaboyer@cnrs-orleans.fr (F.G.)

⁸ Centro de Biología Molecular Severo Ochoa (CSIC-UAM), 28049 Madrid, Spain; mkasma@hotmail.com

⁹ MATIS-Prokaria, 113 Reykjavík, Iceland; viggo@matis.is (V.M.); pauline.vannier@matis.is (P.V.)

¹⁰ Faculty of Food Science and Nutrition, University of Iceland, 101 Reykjavík, Iceland

¹¹ Leiden Observatory, Universiteit Leiden, 2300 Leiden, The Netherlands; p.ehrenfreund@chem.leidenuniv.nl (P.E.); monaghan@strw.leidenuniv.nl (E.M.); riedo@strw.leidenuniv.nl (A.R.)

¹² European Science Foundation (ESF), 67080 Strasbourg, France; PCabezas@esf.org (P.C.); nwalter@esf.org (N.W.)

* Correspondence: garciadl@cab.inta-csic.es; Tel.: +34-91-520-6431

Received: 31 July 2019; Accepted: 16 September 2019; Published: 18 September 2019



Abstract: One of the main objectives for astrobiology is to unravel and explore the habitability of environments beyond Earth, paying special attention to Mars. If the combined environmental stress factors on Mars are compatible with life or if they were less harsh in the past, to investigate the traces of past or present life is critical to understand its potential habitability. Essential for this research is the characterization of Mars analogue environments on Earth through the development of techniques for biomarker detection in them. Biosensing techniques based on fluorescence sandwich microarray immunoassays (FSMI) have shown to be a powerful tool to detect biosignatures and depict the microbial profiles of different environments. In this study, we described the microbial biomarker profile of five anoxic Mars analogues sites using the Life Detector Chip (LDChip), an antibody microarray for multiple microbial marker detection. Furthermore, we contributed to new targets by developing a new 26-polyclonal antibodies microarray using crude extracts from anaerobic sampling sites, halophilic microorganisms, and anaerobic isolates obtained in the framework of the European Mars Analogues for Space Exploration (MASE) project. The new subset of antibodies

was characterized and implemented into a microarray platform (MASE-Chip) for microbial marker searching in salty and anaerobic environments.

Keywords: anaerobic environments; Mars; analogues; biomarkers; microarray

1. Introduction

Searching for life or potential habitable conditions beyond Earth is a central objective in Astrobiology [1–3]. The habitability of early and present Mars has been investigated extensively during the last decades [2–10].

At present, Mars seems to be a dry planet without liquid water on its surface, with an atmosphere mostly composed of carbon dioxide (CO₂) and lacking a significant protecting ozone layer. Thus, the present surface of Mars is exposed to strong UV (ultraviolet) radiation with extremely low temperatures and without liquid water on its surface, although it could exist in the subsurface [7,11–13]. These current conditions make the Red Planet, at first glance, inhospitable for life on the surface, but conditions may have not always been that harsh. Around 4.1–3.7 billions of years ago (Ga), the planet had a thicker atmosphere and moderately stable and warmer surface temperatures, which could have allowed for the presence of liquid water on the surface [14,15]. Moreover, orbital images from Mariner 9 [16] provided the first evidence for past liquid water on Mars, and the Mars Reconnaissance Orbiter [17] showed fluvial features at an ever-increasing resolution, suggesting water flow on the surface of Mars in the past. On the other hand, there are data indicating the possibility of water on the present Mars at the equator where low-albedo features form and grow during the warmer months and disappear in the cold seasons, causing so-called recurring slope lineae (RSL), which could be explained by the existence of liquid brines near the surface; however, this is still an open question [13].

Though the source of water that could be the origin of these features remains unclear, it seems that under certain conditions, small quantities of liquid water, possibly brines, can still form close to the Martian surface under the current climate [13,18,19]. In comparably salty terrestrial environments, different microorganisms can be found [4,20–23], adapted to the high content of salt where the deliquescence of hygroscopic minerals provides liquid water available for microorganisms [4]. Therefore, from the perspective of salt content, the brines on Mars could provide aqueous, highly salty biotopes suitable for adapted halophilic microorganisms [4,21,22]. Geochemical data from Martian meteorites and planetary exploration instruments such as the high oxidant (iron-rich smectite clays, iron oxides, and magnesium sulfate) composition of the surface [24–27] and the cold desiccated radiation-bathed surface of the planet indicate that habitable conditions are most likely restricted to the subsurface rather than on the surface [8,28], where biota, which may have inhabited Mars in the past, were forced to retreat and might still persist today [7]. This retreat could have induced microbial life, if it ever occurred, likely to be more abundant in protective niches far from radiation, desiccation (in brines) and lack of oxygen. This drove us to study the microbial ecology of anoxic analogue environments on Earth, which had been less well investigated up to now, even taking into account that most known extraterrestrial environments are oxygen-free or contain very low abundances of this gas. Though recent studies [29] have suggested that in certain Mars areas, enough oxygen may be available for some microbes to breathe, it is expected that the predominant type of potential organisms would be anaerobes. Precisely, the thin Martian atmosphere contains 0.14% oxygen, and the surface and subsurface of that planet are prone to be suitable for facultative anaerobic and the majority of strict anaerobic microorganisms [30].

The anoxic analogous environments selected show a number of characteristic parameters, such as (i) low water activity, (ii) low temperature, (iii) the restricted availability of (complex organic) nutrients, (iv) oxygen limitation, and other stress factors for microbial life (e.g., high salinity, high acidity, and radiation) [31]. Since the greatest challenge would be to find living organisms on Mars, the

identification of biomarkers from physico-chemical and metabolism processes is a plausible approach. The study of the detection and preservation of microbial biosignatures in anoxic analogous extreme terrestrial environments will broaden our knowledge and improve strategies for the search for potential microbial traces in protective habitats on Mars.

In the framework of MASE (Mars Analogues for Space Exploration), a European Seventh Framework Programme, FP7-funded project, we investigated several anoxic Mars analogues sites, including (i) cold sulfidic springs, (ii) an acidic lake environment, (iii) a hypersaline subsurface environment, and (iv) rock glacier sites in order to obtain a collection of different anoxic samples (soil, water and sediments) that were subjected to a set of investigations. Throughout these investigations by the MASE project team, the whole anaerobic community was characterized by sequencing [31], culture enrichment, and the isolation of microbial strains, which were deposited in the German Collection of Microorganisms and Cell Cultures GmbH (DSMZ, Germany) for long-term storage and distribution to other interested scientists [30]. Studies of physiology, biochemistry, several stress resistance assays, the mineralization of extremotolerant strains from these analog sites and metabolomics studies [32–35] were carried out, as well as the subject of this paper: The search for detectable biosignatures and the description of analogous sites' biomarker profiles.

In the last two decades, several works have proposed immunosensor techniques based on bioaffinity through the use of antibodies for in situ analysis for biomarker detection in planetary exploration [36–39]. One of the most promising analytical methods among them is the Signs of Life Detector (SOLID)-LDChip system [36,38,40] based on a multiplex fluorescence sandwich microarray immunoassay (FSMI), designed for and previously applied in astrobiology studies as well as in microbial ecology studies [40–43]. The LDChip is an antibody microarray-based biosensor for monitoring the presence of microbes and their metabolic products in different kinds of environmental samples. It was developed and implemented for in situ detection of biomarkers and it is the core sensing device of the SOLID instrument [40]. The LDChip has been used for detecting prokaryotes' biomarker profiling in different extreme environments, which include the acidic iron-rich sediments of Rio Tinto in Spain [44–46], subsurface sediments cores in the hypersaline Atacama Desert [40], the surface and sediments drilled on Deception Island in Antarctica [47] and Andean glacial lakes [43,48].

In this article, we report the heterogeneity of the microbial profiles of a whole set of samples from the Mars analogues characterized by MASE team by using the LDChip. Additionally, and as a direct output of MASE microbial isolates, this study contributes with a new set of microbial targets and antibodies from anaerobic and halophiles microorganisms for biomarker detection. This can be used to implement a new LDChip for planetary exploration. The new LDChip proposed here (MASE-Chip) consists of 26-polyclonal antibodies against the mentioned halophiles and MASE anaerobic isolates.

2. Materials and Methods

2.1. Mars Analogues Selection and Sampling

Since none of the terrestrial Mars analogue environments possess all Martian stress factors at once and in the same location, the selected MASE sites—taken in combination—are a good representative of not every but a desirable range of conditions on Mars throughout its history [30]. The MASE sites share some characteristics that were used as criterion for their selection: (i) They are limited in nutrients, (ii) anoxic in nature, and (iii) correspond to a particular postulated environment representative of past or present-day Mars. The MASE sites where sampling was carried out are the following:

- Boulby mine in the United Kingdom (UK), a potash mine one kilometer deep in the north-east of the UK that contains sequences of Permian halite and sulfate deposits [49] with anoxic conditions inside [50]. The physicochemical characteristics of ponds in Boulby (salt-saturated, pH neutral, subsurface bodies of water that host anoxic environments in their sediments) provide an environmental analogue to potential water bodies that may have existed in Martian evaporitic water [51,52].

- Gränavatn Lake in Iceland, one of several lakes in the geothermal area of Krýsuvík that originated from volcanic explosion craters [53]. The near-lakeshore environment is characterized by periodic desiccation and an acidic pH, with volcanic rock-water interactions and low water temperatures. This makes it a Mars analogue of deltaic deposits found, for example, at Jezero Crater, which closely resemble those found in terrestrial lacustrine settings [54,55].

- Regensburg in Germany, where many anoxic sulfide-containing springs emanate from the subsurface. Two of them have previously been studied at the Sippenauer Moor and Islinger Mühlbach areas [56–58]. Both are characterized by a main sulfidic spring that rises into a streamlet where whitish mats of sulfide-oxidizing bacteria cover the submerged surfaces. These aquifers are very similar to sulfidic cave springs that are rich in sulfide, ammonia and sulfate but poor in dissolved organic carbon. The Sippenauer Moor and Islinger Mühlbach sites are independent, and they are not connected in the deep subsurface, even though they both emanate from Mesozoic sediments formation and are fed by the same deep groundwater flow within the pre-alpine Tertiary Molasse basin [59,60]. The domination of the sulfur cycle on Mars [61] makes these aqueous environments that contain diverse sulfur species useful potential analogues.

- Kaunertal, Austria: The edges and bedrock of glacial environments offer the possibility of collecting samples from perennially frozen soils and ices. Glacier samples were collected from a rock glacier in the Kaunertal, Austria, in the frame of the Austrian Space Forum's AMADEE-15 analog program. The Kaunertal valley is 28 km in length and runs southeast from the town of Prutz to the Kaunertal Glacier. Samples of soil were taken from the glacier and from a streamlet derived from melted glacier ice [30].

In summary, sediments and water were sampled from all MASE sites. In Boulby (hypersaline environment), two different brine seeps were sampled at the Billingham Bath location (samples referred to as Bou.I and Bou.II hereafter; coordinates: 54.5575; −0.8202 in mine surface). These sites were located ~14 km distance from the coastline under the North Sea. Regarding sulfidic springs (Regensburg), samples were taken at two different sampling locations in Regensburg at Sippenauer Moor (SM) (sulfidic spring SM, coordinates 48.8685; 1.9563) (water (SMw) and sediment (SMs) samples), and at Mühlbacher Schwefelquelle Isling (MSI) (sulfidic spring MSI, sediment sample, coordinates: 48.9857; 12.1272). In Iceland, samples were extracted in anoxic conditions at two different sampling sites at Gränavatn Lake (Icelandic acidic lake) (IS.SS1, coordinates 63.8857; −22.0544 and IS.SS3, coordinates 63.8830; −22.0565). Finally, Glacier samples were collected from a rock glacier in the Kaunertal, Austria (Glacier) (samples named G. ss1 I, G. ss1 II, G. ss2 I, G. ss2 II according to sample sites 1 or 2 and duplicates in each site, I and II).

To ensure sampling in anoxic conditions, the field equipment included, among others, Duran glass bottles medium sealed with a rubber bung and a screw cap containing anoxic atmosphere. As reducing agents, aliquots of filter sterilized cysteine-HCl (50 mL of 2.5% w/v) were used to adjust the anoxic atmosphere, and resazurin (20 mL of 0.1% w/v) was used as a redox-indicator. Syringes, cannulas, wipes soaked in ethanol and other components were used for the sampling. The detailed list and procedure that could be broadened in [30] included previous steps to prepare the sampling anaerobic glass bottles as follows: 0.5 mL of a resazurin solution (a redox-sensitive dye to monitor redox potential) were pipetted into each 100 mL Duran laboratory bottle. Subsequently, the bottles were closed with a butyl rubber stopper, which was held in place with an appropriate screw cap. This step was followed by three gas-vacuum exchange cycles using nitrogen in order to obtain an oxygen-free atmosphere within the bottle. The last step included purging with nitrogen until an overpressure of 0.2–0.5 bar was reached. Once this was done, the bottles were autoclaved for 40 min at 121 °C.

The sampling procedures followed the subsequent steps: Prior to the removal of the screw cap and the rubber stopper, the overpressure within the anaerobic Duran glass bottle was removed by the use of a sterile needle. The butyl rubber septum was sterilized using ethanol. The sediment and water samples were taken the corresponding pool in each case as deeply as possible (approximately 30–40 cm below the water level in Boulby and Gränavatn using a sterile Falcon tube that was attached to the end

of a pole and 20–30 cm below the water level in the sulfur springs of Regensburg using anaerobic glass bottles). Once the rubber stopper was aseptically removed, the sediment was immediately poured into the glass bottle and filled up to the brim with site water that was also collected. After filling the bottles with sediment, brine or water, they were closed with the rubber stopper. The last step included the addition of the reducing agent mentioned (1 mL cysteine-HCl of a 2.5% solution) to depress and poise the redox potential at optimum levels. In every moment, the highest care was taken to keep samples away from contamination and to minimize oxygen, possible traces of which were quickly removed by the methods indicated before.

Samples were taken in three replicates of 100 mL bottles to distribute them among the team for each purpose and stored at 4 °C until their use.

2.2. Immunoprofiles of MASE Sites Using Fluorescence Sandwich Microarray Immunoassays

The different samples described were analyzed by a sandwich microarray immunoassay through a 168 antibody-containing LDChip. This LDChip includes antibodies against (i) whole microbial cells representatives of the main phylogenetic groups of prokaryotes/archaea, (ii) extracellular polymers, (iii) environmental extracts from terrestrial analogues for Mars, (iv) proteins and peptides from well-conserved anaerobic metabolic pathways, (v) exopolysaccharides, and (vi) amino acids, among others biomolecules used in metabolism. The antibodies printed in the mentioned chip were performed in rabbits from samples in the list below. The immunoglobulin-IgG-fraction of each antibody from the rabbits serum was purified with protein A and spotted in triplicates over the surface of epoxy-activated glass slides (Arrayit, CA, USA) [36,62] (Table S1). Over the explained LDChip, the sandwich immunoassay with the MASE site samples (Figure 1) was carried out, adapted from the procedure described previously in [36,62]. This consisted of an ‘antibody-antigen-labelled antibody’ (Ab-Ag-Ab*) bound where the antigen comes from the extraction of epitopes from samples using 2 g (for sediment samples) or 50 mL (in the case of water samples) of each one. These epitopes were obtained by sonication of the samples (3 cycles of 30 s at 90% maximum amplitude on ice; DR. Hielscher 50W DRH-UP50H sonicator, Hielscher Ultrasonics, Berlin, Germany) in a buffer extraction (NaCl 0.3M, Tris-HCl 0.4 M pH = 8, 0.1% Tween 20) and filtered through a 5 µm nylon membrane to remove possible minerals and coarse material.

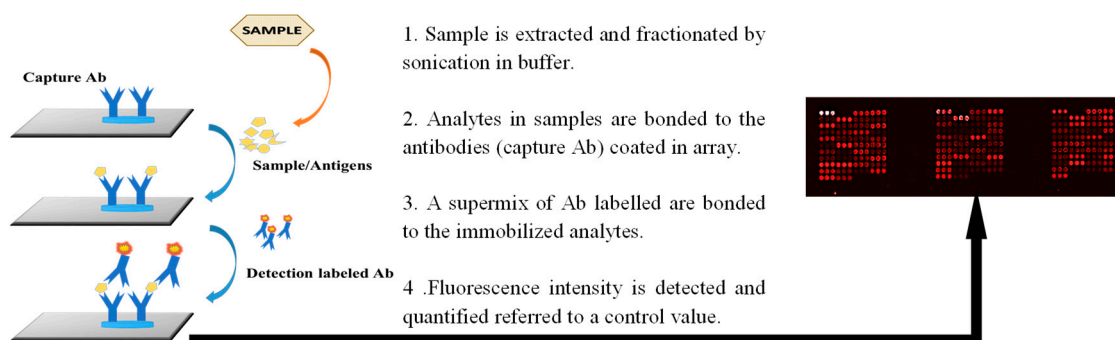


Figure 1. The scheme of the sandwich immunoreaction occurring in each spot printed in the microarray with the main steps of the procedure. The image on the right is an example of one of the nine arrays in the slide. Red spots (printed in triplicates) indicate the recognition of epitopes in the sample between the antibodies fixed in the slide and labelled antibodies in the supermix.

First, and prior to displaying the sample, the microarrays were blocked in two sequential steps of 2% and 5% BSA (bovine serum albumin) in a Tris-HCl buffer to minimize unspecific joints. Then, the samples were incubated over the LDChip for 1 h at room temperature to allow for interactions between the capturing antibodies (antibodies spotted in the microarray) and molecules present in the sample. This was carried out inside a MultiArray Analysis Module (MAAM), in which up to nine assays can be processed at the same time [63]. Afterwards, a washing step in which the buffer removed the excess of

the unbound sample occurred. Then, the microarray was incubated for 1 h with an Alexa Fluor-labelled mixture of the same kind of antibodies (Abs) coated in its surface (reporting Abs), resulting in a sandwich conformation (Figure 1). The excess of labelled antibodies—those not bound—was washed, and the slides were scanned with a red laser (635 nm) that excited the reporting Abs.

The fluorescent signal can be captured by a highly sensitive CCD (charged-coupled device) detector and stored as a Flexible Image Transport System (i.e., .fits) image file that could be processed and analyzed by conventional microarray software. Thus, after the immunoassay were completed, and the slides were analyzed in the laboratory by illuminating them with 635 nm light and imaging their fluorescent emission at 650 nm with a GenePix 4100A scanner. The images were quantitatively analyzed using GenePix Pro software (Genomic Solutions). A blank was always run in parallel with only a buffer as the “antigenic” sample and then revealed with the same fluorescent antibody or antibody cocktail as the real samples. This image was used as a baseline to calculate spots intensities in the tested sample. The final fluorescence intensity (F) for each antibody spot was calculated with the equation $F = (F_{\text{sample}} - F_{\text{blank}} - 2.5F_{\text{avcontrol spots}})$, where F is the fluorescent intensity at 635 nm minus the local background, as quantified by the software (GenePix Pro); F_{sample} is the total fluorescence signal of the sample; F_{blank} is the total fluorescence signal of the blank; and $F_{\text{avcontrol spots}}$ is the average fluorescent signal of the control spots. These control spots are located in different parts of the microarray and consist of BSA, the buffer, and spots corresponding to the pre-immune antisera (more than 50). Because, theoretically, they should not exhibit any fluorescent signal, they were used as a baseline for fluorescence. Therefore, 2.5 times the $F_{\text{avcontrol spots}}$ was used as a stringency cutoff to minimize false positives, taking those above this value as real positives. The spots with obvious defects (missing or very tiny spots or an artifact due to a bad wash or dust in the array) or duplicated spots whose standard deviation was 0.2 times higher than the mean were not considered for quantification [40]. The positives fluorescent signals quantified were plotted as an immunogram (Figure 2).

2.3. Building a Microarray from MASE Sites and Salty Environments

In this study, a 26-polyclonal antibody microarray to MASE isolated strains was developed using samples from the sampling sites described, isolated strains from these sites, and was complemented with antibodies from previous studies (Table 1).

Thus, antibodies obtained from 15 isolated microorganisms from MASE sample sites and a set of 11 antibodies available from Molecular Ecology Laboratory (Centro de Astrobiología-CAB, Consejo Superior de Investigaciones Científicas-Instituto Nacional de Técnica Aeroespacial, CSIC-INTA, Madrid) collection of halophilic microorganisms were used to develop and build a new microarray for Mars analogue environment monitoring. Firstly, the 15 isolates representative from MASE sites were selected to immunize rabbits and obtain polyclonal antibodies (against the antigenic fraction), and these were carried out by Biomedal Company and the Immunology Department at Hospital Fundación Jiménez Díaz in Madrid. The used antigens were prepared from isolated bacteria homogenates that were washed three times in PBS by centrifugation for 10 min at 13,000 rpm and then ultrasonicated (4 cycles of 30 s at amplitude of 90%, stopping 30 s on ice between cycles) and filtered by a 5 μm membrane before being injected into rabbits. Secondly, after six weeks of immunization, the IgG fraction of the antibodies performed and recovered from rabbit serum were purified by protein A affinity columns (Sigma). Finally, the set of purified antibodies were fluorescently labelled with Alexa 647 fluorochrome at a concentration of 2 mg mL^{-1} , as recommended by the provider (Molecular Probes, Invitrogen) to be used as the tracer antibody in the sandwich immunoassay. The other set of the same non-labelled antibodies were printed in a triplicate spot pattern on epoxy-activated glass slides as the capture antibodies for the samples/antigens.

In addition, control spots containing only BSA, the buffer and a serial dilution of fluorescent labelled pre-immune antiserum were also printed to be used as baselines and to subtract their average fluorescence from the sample's readings. These fluorescence spots of pre-immune antiserum were also used as indicators of the frame of each individual array to ease the image analysis after its recording.

This microarray, MASE-Chip, was printed in a 3×8 (3 in each row and 8 in each column of the chip surface) array setting in order to be available for 24 different assays at the same time.

2.4. Testing and Validating the New Antibodies and MASE-Chip

As a first step for examining the accuracy of the MASE-Chip and to set the optimal assay conditions to be used in future experiments, two types of assays were carried out with the new antibodies from the MASE isolates generated in this study. These two assays were used for testing both the more efficient concentration of each labelled antibody and the minimum concentration of antigen that could be detected by the microarray. In the first place, a fixed concentration of the antigen was used, and that of its corresponding fluorescent antibody was applied in serial dilutions (from 1/500 to 1/5000) to set the best working concentration. Once the concentration of the labelled antibody was established, the concentration of the antigen was varied until the detection limit was determined from the analysis of the images corresponding to different dilutions, providing calibration curves. Accordingly, the cross reactivity, and therefore the specificity, could be revealed, allowing us to disentangle the potential points of non-specificity of the microarray to be taken into account in further experiments. The analysis procedure to determine the positive immunodetections by the immunogens and antibodies followed the same principles described before for the generation of immunoprofiles by means of fluorescence signals over a cutoff value.

3. Results

3.1. Biomarker Profiles of MASE Sites

Anaerobic water and sediment samples from each selected MASE site (Regensburg, Germany; Gænavatn Lake, Iceland; Boulby Mine, UK; and Kaunertal Glacier, Austria) were processed in the laboratory by sonication (material and methods section) to obtain the extracts or epitopes that were analyzed using the LDChip, which included different antibodies (small peptides and molecules, proteins, exopolysaccharides and cell extracts; Table S1). The fluorescent images obtained from the assay were analyzed, and the fluorescence intensity of each antibody spot on the microarray was quantified. Data from this analysis were plotted as immunograms or biomarker profiles (Figure 2). The immunograms showed several positive antigen-antibody signals in all the samples analyzed: Boulby Mine—hypersaline environment (Bou. I and II); Gænavatn Lake—acidic lake (IS.SS1 and IS.SS3); Regensburg—sulfidic springs (SMw, SMs and MSIs); and Kaunertal Glacier, Austria—glacier (G.ss1-I, G. ss1-II, G. ss2-I, G. ss2-II). In this way, Figure 3 depicts the results from the immunoassays of each sample/sample site on a heat map (number of positive hits and relative abundance), where differences regarding detectable biomarkers in relation to phylogenetic groups can be seen and provide useful information about the microbial community. Table S1 in Supplementary Materials lists the antibodies in the LDChip, those detected in these positive immunodetections, the source and the immunogen of each one, and their cluster, phylum, and reference.

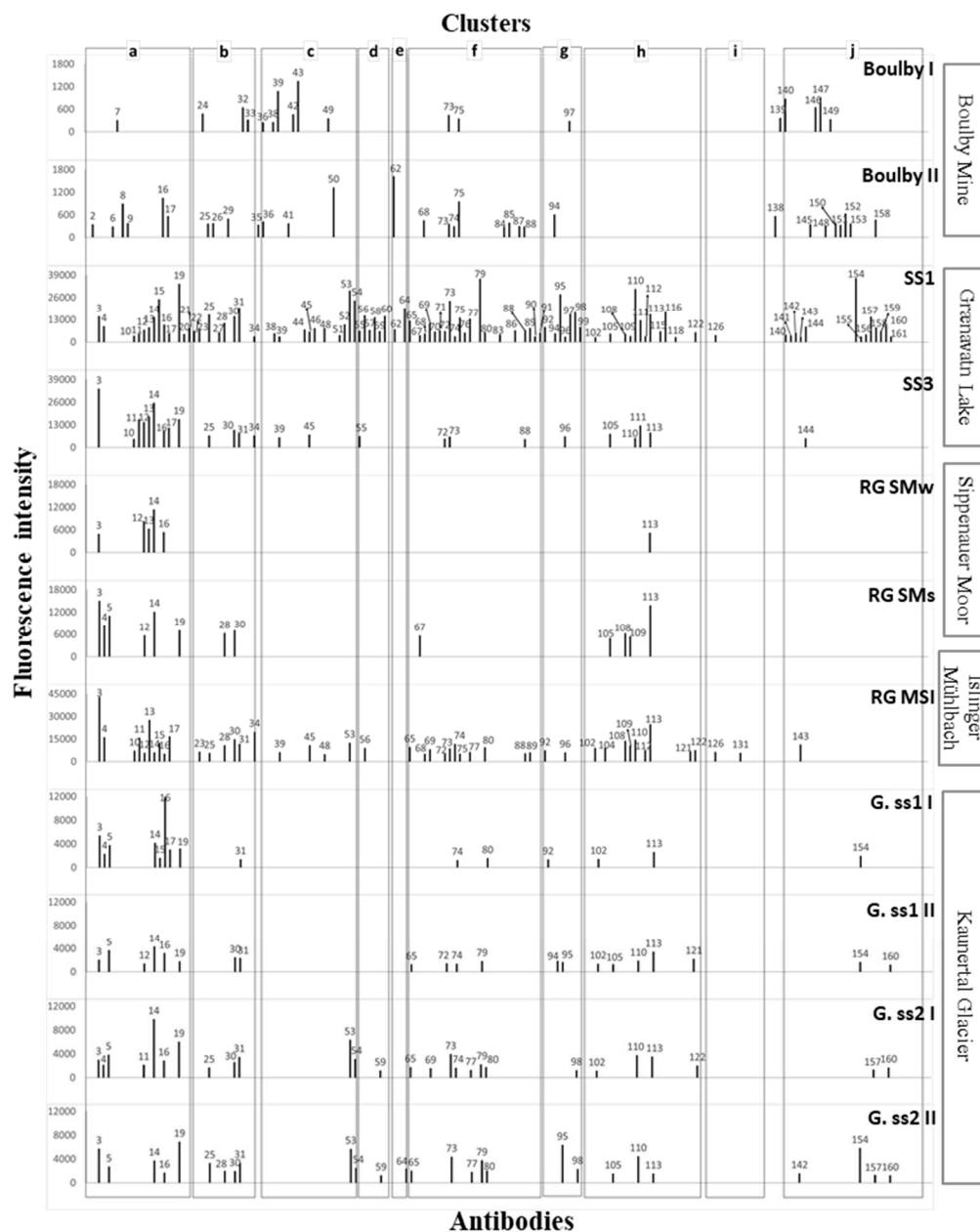


Figure 2. Immunograms of water and sediment samples of each Mars Analogues for Space Exploration (MASE) site (explained in Material and Methods section). Plots show the positive immunodetections and their fluorescence intensity. The peak numbers correspond to the antibody detected in each reaction and are listed in Table S1. Letters above from **a** to **j** frame those antibodies of positive immunodetections that has been clustered as follows: **a.** Fe-S oxidizers cultures; **b.** metal-acidic environment (water source); **c.** psychrophilic cultures; **d.** iron reducers; **e.** spores; **f.** mesophilic cultures; **g.** archaea; **h.** cyanobacteria; **i.** perchlorate reducers; and **j.** proteins and peptides. Moreover, some groups are represented by a sole antibody: Peaks 35, Ab ID: IIC1C1 geothermal environment; 138, Ab ID: VIID1BF, mesophilic environment; and 139, Ab ID: VD2BF, biofilm from mines. Please note that scales of the Y axes (fluorescence intensity) are not the same for every site, but they remain homogenous within each one.

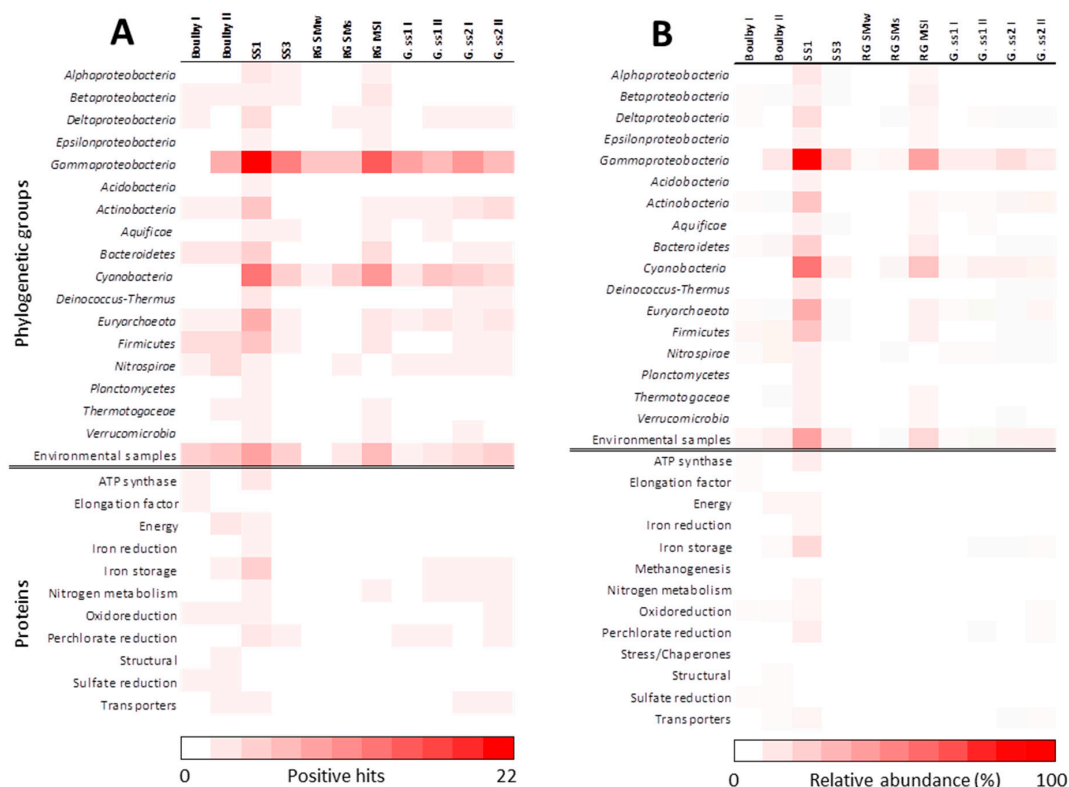


Figure 3. Heat map showing the results obtained with the Life Detector Chip (LDChip)168 immunoassay in samples from MASE sites (Boulby I (Bou-I) and Boulby II (Bou-II) from Boulby Mine (hypersaline environment); IS.SS1 and IS.SS3 from Iceland-Grænvatn Lake (acidic lake); RG. SMw (water) and RG. SMs (sediments) from Sippenauer Moor (sulfidic spring SM); RG. MSI from Islinger Mühlbach Schewefelquelle (sulfidic spring IM); and G.ss1-I, G. ss1-II, G. ss2-I, G. ss2-II from Kaunertal Glacier, Austria (glacier). The antibodies that showed positive immunodetections were clustered by phylogeny of the targets, protein function, or environmental origin and plotted in a scale from white to red. (A) The number of hits is represented from 0 to 22, as the maximum number of hits of antibodies (Abs) from the same group detected in a sample. Here, certain underestimations may result from representing the positive immunodetections in those groups with a lower number of antibodies represented in the chip. In (B), the number of hits was normalized by the relative weight of each group represented in the chip and expressed as the relative abundance in percentage. The immunoprofiles of the samples did not change substantially with the normalization, but the intensities of detection decreased in terms of abundance. Total antibodies showing positive immunodetections appear in Table S1, marked with “+,” where the identification code of the antibody detected, their immunogenic fraction, and the sources (environmental sample or microbial strain) used for its production are also indicated.

The results revealed a high heterogeneity of the different samples and sites. In some cases, even in the same site, heterogeneity was observed between samples from different locations, as was the case of Grænvatn Lake and in the two sulfur springs in Regensburg. Notwithstanding, a common feature of all of them was that the main phylum detected by the antibodies, corresponding with the majority of the positive immunodetections, was Gammaproteobacteria, which showed a wide presence in almost every sample except for Bou. I (Figure 3).

The highest detection in the number and diversity of biomarkers through the LDChip168 appeared in the SS1 sample from Iceland (Grænvatn Lake) and in the sediments from the MSI sulfidic spring in Regensburg (Figures 2 and 3). In contrast, the lowest detection of positive signals, regarding number and diversity, was found in sample site 1 from Kaunertal Glacier (G.SS1), in the water sample from Sippenauer Moore sulfidic spring (RG.SMw), and even in the sediments of this sulfidic spring (RG.SM). Though the hypersaline environment (Boulby) showed lower intensities than the rest of the samples in

terms of relative fluorescence, the number of biomarkers detected was higher (Figure 3). Furthermore, the strongest fluorescence intensities appeared in sample 1 from Iceland (IS.SS1), with the exception of peak 3 in RG.MSI, where the highest peaks corresponded to antibodies raised against the iron-sulfur reducers (peak 19), psychrophilic cultures (peak 53), mesophilic cultures (peak 79), archaea (peak 95), cyanobacteria (peaks 110 and 112) and proteins and peptides (peak 154) clusters.

Contrary to what one might initially expect due to the cold nature of the environment, positive signals for psychrophilic-source antibodies were rarely found in the glacier samples of the current study, but several positive immunodetections belonging to the mesophilic cluster were present. Within this mesophilic cluster, relatively significant phylum diversity could be appreciated (Figure 2, column f), especially in G.SS2 samples. In general, both sample sites from Kaunertal Glacier displayed low intensities in fluorescence signals compared with the rest, but they were still higher than those from Boulby.

Interestingly, apart from being the richest in terms of number and types of detectable biomarker signals, the immunopatterns of IS.SS1 (acidic lake) and RG.MSI (sulfidic spring) were notably similar, with the exception of antibody signals coming from proteins. These were present in the lake samples but were not traceable in the sulfur-spring sediment. Nevertheless, the intensities of the peaks in Regensburg samples were lower than those from Grænavatn Lake, except for peak 3, which corresponded to the antibody named A183 taken from *Leptospirillum ferrooxidans*.

As part of another study from MASE project about the microbial communities thriving in the MASE sampling sites [31] the German–Austrian group of the MASE team provided metagenomic data based on 16S rRNA gene amplicon and shotgun metagenome sequencing. The study was carried out by discerning sets of total bacterial and those living in the sample by the use of a DNA-intercalant: Propidium monoazide (PMA) that is a membrane-impermeant dye that intercalates into the DNA and distinguishes cells with compromised membranes from those intact (live) cells. [64]. Therefore, samples treated and untreated with PMA and subjected to metagenomics analysis by a universal primer set [31] showed some slight differences each other (Figure 4). Though these results, compared with the LDChip analysis (Figure 4), disclosed a moderate coincidence between relative abundance of sequences identified by metagenomics and the relative abundance of biomarkers detected, the high abundance of signals of Proteobacteria detected by both methods is still remarkable.

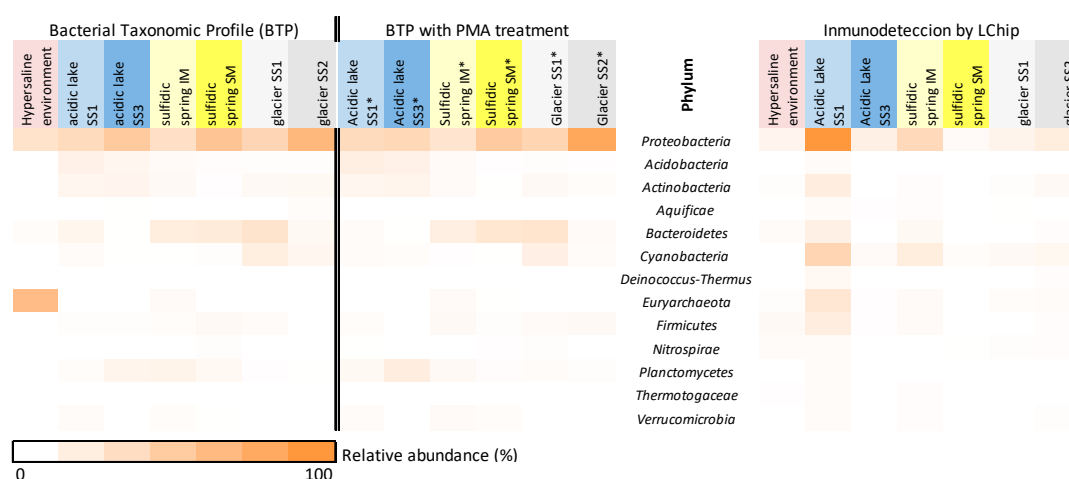


Figure 4. Comparison of bacterial abundance of the samples at phylum level. The heat maps display the relative abundance of phylum in each sample, where left panels show the universal primer set approach (samples without propidium monoazide (PMA) treatment and with PMA treatment-marked with asterisk*) and the right panel, the positive immunoreactions by the LDChip. Hypersaline environment: Boulby Mine (Bou); acidic lake SS1 and SS3 (Grænavatn Lake, IS.SS1 and IS.SS3); sulfidic spring IM and SM (Regensburg, RG.SM and RG.MSI); Glacier SS1 and SS2 (Kaunertal Glacier, G.SS1 and G.SS2). Sequences from hypersaline environment were not available for PMA treatment due to the interferences between salts and PMA [65].

3.2. MASE-Chip

The LDChip results showed the presence of certain microbial groups and suggested different potential metabolic activities in the collected samples. Because of the inherent limitations of the LDChip due to its limited number of antibodies (168 in this case), we could not rule out the possibility of failing in the detection of a high number of microorganisms due to the absence of the appropriate antibody. Therefore, we contributed to enlarge antibodies collection for these Mars analog sites and prepared antibodies to a collection of 26 environmental isolates (Table 1) from the different MASE sites and from an existing antibodies' collection from Molecular Ecology Laboratory (Centro de Astrobiología-CAB, CSIC-INTA, Madrid). We tested and implemented them in a microarray chip, the so called MASE-Chip. We determined the optimal working concentration of the labelled antibodies and the specificity to assess the accuracy of the microarray following the procedures explained before in the Materials and Methods section. The working dilutions ranged from 1/800 to 1/900, and the lower detection limit of most of antibodies was established between 10^4 and 10^3 cells mL⁻¹ (details of each antibody in Supplementary Materials, Table S2).

Table 1. Antibodies printed in the MASE-Chip with their IDs (left column), their immunogen source, and their references (up: Unpublished). The first 15 of them came from isolates of MASE project and the rest belong to the Molecular Ecology Laboratory antibody collection at CAB.

Ab Name/ID	Immunogen (Sample/Strain)	References
Bou. I	Boulby Mine I (wet and pink salt)	-
Bou. II	Boulby Mine II	-
MSIs	Mülbach Islinger-Regensburg (cold spring-sediment)	-
SMs	Sippenauer Moore-Regensburg (cold spring-sediment)	-
IS. SS1	Grænavatn Lake-Iceland (sediment)	-
MASE-BB-1	<i>Halanaerobium</i> sp. (isolate from Boulby)	[30]
MASE-IM-5	<i>Trichococcus</i> sp. 37AN3 (Mülbach Islinger)	[30]
MASE-IM-4	<i>Clostridium</i> sp. DSM632 (Mülbach Islinger)	[30]
MASE-SM-3	<i>Hafnia</i> sp. (Sippenauer Moore)	[30]
MASE-SM-2	<i>Clostridium</i> sp. (Sippenauer Moore)	[30]
MASE-SM-1	<i>Methanomethylovorans</i> sp. (Sippenauer Moore)	[30]
MASE-IM-7	<i>Desulfovibrio</i> sp. (Mülbach Islinger)	[30]
MASE-LG-2	<i>Pelosinus</i> sp. (Grænavatn Lake)	[30]
ET2	<i>Bacteroides xylophilus</i> X5-1 (Grænavatn Lake)	up
MASE-Glacier-SS3	<i>Rhanelia</i> sp. (Kaunertal Glacier)	[30]
IVE7C1	<i>Halothiobacillus neapolitanus</i>	[40]
IVG5C1	<i>Sulfobacillus acidophilus</i>	[40]
IVI12C1	<i>Geobacter metallireducens</i>	[62]
IVI20C1	<i>Salinibacter ruber</i> M8	[40]
IVI21C1	<i>Salinibacter ruber</i> PR1	[40]
IVI24C1	<i>Thessaracoccus lapidicaptus</i>	[66]
IVJ1C1	<i>Haloferrax mediterranei</i>	[62]
IVJ8C1	<i>Halorubrum</i> sp.	[40]
IVJ9C1	<i>Halobacterium</i> sp.	[40]
IVK19C1	<i>Chroococcidiopsis</i> O29	up
VD2BF	Biofilm from Mansimongs Mines Southafrica	up

From these analyses, we established the cross-reaction occurring in the MASE-Chip so that we could use this information to distinguish true antibody-target from other specific interactions due to shared antigens and discern false positives when analyzing a complex or environmental sample

through it. These cross-reactions in the FSML, and therefore the specificity of each Ab, were revealed by the positive immune detection measured and quantified through their relative fluorescence intensity in each case. The qualitative results are shown in Figure 5 as a heat map of the positive immunodetections and a diagram mapping the cross-reactions occurring in the MASE-Chip.

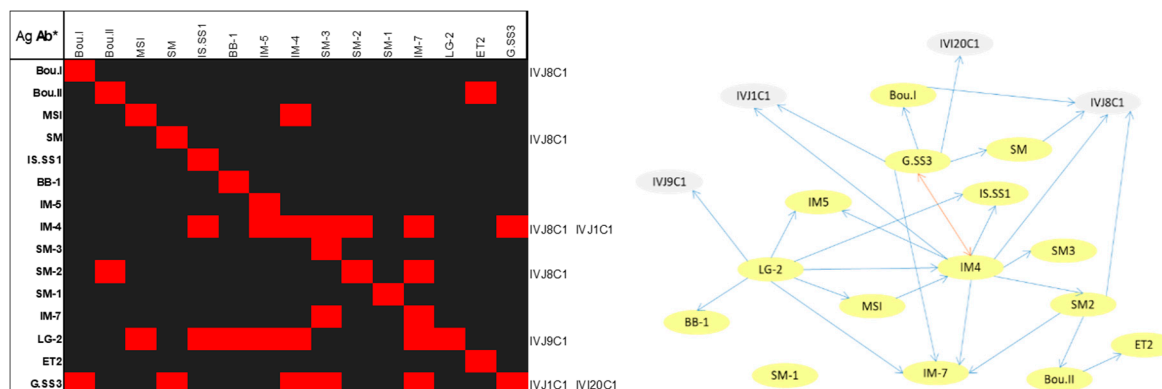


Figure 5. Cross-reactions in the MASE-chip. The heat map on the left shows the positive immunodetections (red squares) of the sandwich immunoassay *Ab capture-Ag-Ab trace* (*labelled). In the vertical left column, the tested antigens (so they are in rows) are represented. The top line of the table indicates Abs labelled (in columns). The outside column in the right part of the heat map shows the capture Abs printed on the array from previous collection and used in the building of MASE-Chip that cross-react and recognize MASE targets. The image on the right qualitatively shows the cross-reactivity events revealed in the heat map, where yellow circles represent the new Ab from MASE isolates, and the grey ones represent the Ab taken from previous studies. The blue arrows show the recognition of an Ab for the immunogen indicated. The orange arrow represents double direction recognition as happens between G.SS3 and IM-4 antibodies. The self-loops were not drawn to improve the clarity of the image. (The length of arrows is not informative of quantification).

The results indicate that in several cases, the antibodies from the new MASE isolates were specific for their corresponding immunogen targets, although some were also captured by other antibodies on the microarray that came from a previous antibody collection. This occurred in the following cases: Bou.I, SM, IM-4 and SM-2—these immunogens also reacted with antibodies to *Halorubrum* sp. (IVJ8C1). Antibodies to *Haloferax mediterranei* (IVJ1C1) recognize IM-4 and G.SS3 antigens; antibodies to *Halobacterium* sp. (IVJ9C1) and to *Salinibacter ruber* M8 (IVI20C1) bound to LG-2 and G.SS3 immunogens, respectively. The highest cross-reactivity among the MASE antibodies identified was shown by LG-2, IM-4 and G.SS3. Noticeably, some Abs tested in the microarray recognized more than the one antigen that originated from them.

4. Discussion

Previous studies have extensively demonstrated the potentiality of LDChip technology, in its different versions, in several environments, such as the Atacama Desert, Glacial Lakes, acidic Rio Tinto River, permafrost in Antarctica, or deep South Africa Mines [40,47,48,62,67] as a reliable tool for environmental monitoring and profiling biomarkers and natural microbial communities present in ecosystems. Herein, we again demonstrated the potentiality and the ability of LDChip technology for a rapid assessment (a few hours) of the microbial profile of environmental crude samples in anoxic environments and its potential for biomarker detection in planetary exploration.

Regarding the studied biomarker profiles and taking into account not a phylogenetic criteria but a temperature tolerance as condition one, we identified a great absence of signals to antibodies from psychrophilic strains in contrast with the high number of those from mesophilic environments in the case of the glacier samples (Figure 2). The type of samples in this site, which were soil, could be prone to experiencing temperature fluctuation cycles to which mesophiles are better adapted [68].

In addition, although some studies have claimed that psychrophilic microorganisms are presumed to be predominant in those areas and niches permanently freeze [69], others have indicated the higher relative abundance of psychrotolerants and mesophiles over the amount of psychrophiles [70,71]. The absence of positive signals belonging to antibodies from psychrophilic bacteria in the samples of this study possibly responds to the fact that mesophilic biomass could be, as mentioned before, more abundant and could be better adapted than psychrophiles, causing a relative screening effect in biomarker detection. Another contribution to these results is the nature of the LDChip, which, although presenting a relatively similar number of antibodies of each group (19 from psychrophiles and 27 for mesophiles), detected antigenic determinants that could be shared by psychrophiles and mesophiles that were genetically related. Nevertheless, in glacier sample site 2 (G.SS2), biomarkers, of which sources were the psychrophiles *Psychrobacter cryohalolentis* (IVF8C1, peak 54 in immunogram Figure 2) and *Colwellia psychrerythraea* (IVF7C1, peak 53) were still perceptible, and the last one is considered as a facultative anaerobe that seems to adapt to cold environments by the production of extracellular polysaccharides [72].

In addition, among the samples, IS.SS1 from Grænavatn Lake displayed a large number of different biomarkers and presented the highest intensities in their fluorescence signals, where almost all phyla available in the LDChip were represented. Diversity data from MASE team studies on microbial community in MASE sampling sites [31], although with lower relative abundance and intensities, have been quite consistent with these findings and have shown a reasonable range of bacterial composition in sample IS.SS1 using a universal primer approach. Samples from Grænavatn Lake, especially IS.SS1, showed the prevalence of signals of antibodies from sources of metal-acidic environment, iron oxidizers cultures and acidophilic strains clusters that indicate the presence of this kind of molecular biomarkers or microorganisms from these groups or both [40]. The findings are relevant to this acidic lake, which is subject to periodic desiccation and has volcanic rock–water interactions [53]. These characteristics, in general, occur in the anoxic environments of Iceland and constitute sustained bodies of liquid water interacting with volcanic bedrock and with few other rock types represented; thus, these could be a potential analog for early Martian environments [73].

Regarding the sampled sulfidic springs sites (Regensburg), the RG.MSI sample seemed richer than the samples from RG.SM, which was probably due to the retention effect of sediments. These sediments retain organic compounds and nutrients, acting as a filter for water and, at the same time, constituting a nurturing enriched matrix that can serve as a favorable niche for microbes [74,75]. In this way, the water, apart from being a natural diluent of nutrients by itself, in these sites, is sieved by the sediments, which could explain the lower detection of biomarker signals in number and intensity.

Positive signals from those antibodies against proteins and peptides were more strongly detected in the salty environment and in the acidic lake in Iceland. This could provide clues about the kind of metabolism that could be occurring in the niche involving nitrogen and sulfate reduction (NRA, Prot_ApsA_RB11754, Prot_DsrA_RB11365, Prot_DsrB_RB11368, NirS, NOR1), synthesis of ATP (ASB, ASF1) and iron metabolism (Prot_FeReTs_983, Prot-Pfu-FER), among others (IDs of Abs in parentheses, see Table S1). Recent works using LDChip technology [43] have reported the presence of a rich microbial community in the shallow sediments of the lake shore of glacial lakes which may constitute a variety of anaerobic metabolisms. These kinds of metabolisms could have been occurring in the anoxic sites of this study in which similar positive signals have been detected by the immunoassays.

In the particular case of hypersaline samples, although there was a qualitative correlation in terms of some phylum clusters detected (Euryarchaeota, Bacterioidetes, and Proteobacteria) between biomarker and biodiversity data, some phylum which were also detectable by the chip were not identified by metagenomics (Actinobacteria, Firmicutes and Nitrospirae). It was observable that the proportion of each one in those detected by both approaches stayed different and that the positive signals obtained from microarray seemed lower especially for Proteobacteria. This deviation may have been caused by a disturbance over experimental procedures of the high salt concentration in samples, even though assay protocols were optimized to minimize these effects. Nevertheless, although the

“salty-effect” caused a decrease in the intensity of the signals detected by the LDChip, the phylogenetic diversity of the biomarkers detected by this method remained higher. There was a relative bias regarding the nature of the antibodies printed in the LDChip168 due to different proportions of each group represented and because it did not cover the whole microbial diversity (Table S1). This could be the reason for the certain lack of correlation with DNA data, not only in these samples but also in the rest of the samples of this study (Figure 4). In addition, it is worth noting that the MASE site samples were subjected to microscopy examinations by the MASE team, which revealed a low amount of microbial cells, as well as abundant particles [31]. This probably caused certain metagenomic biases regarding DNA extraction and the sequencing process. It would be the responsible for certain deviations in data correlation between the LDChip and metagenomics in some samples regarding the less abundant phylums. This did not sufficiently affect in the case of the Proteobacteria phylum, members of which were widely identified by sequencing, and biomarkers from sources of it (46 antibodies among the total 168 antibodies in the LDChip) were detected by the LDChip for all the samples studied.

Nevertheless, taking data in combination, there was a grade of correspondence and mainly a complementation in the diversity of phylum in the Boulby samples and in the rest of the MASE sites, as well as the diversity in biomarkers detected by immunoassays. This, together with previous studies in which correlations between these techniques were relatively higher than in the MASE sites but still not absolutely coincident [40,43], supports the microarray approach as a reliable tool for biomolecules detection. Moreover, it drives the continuation of the development of specific microarrays for distinctive and particular features of environments using antibodies from sources of those features and adaptations.

In general, based on the comparison of the two molecular approaches, the metagenomics analysis, and immunoassays with the LDChip, we could conclude, once again, that the LDChip is a highly useful immunosensing technique for biomarker and microbial detection which successfully complements and adds to the information obtained by classical techniques and with a desirable potential for planetary exploration. The power of this technique was recently proven for Mars exploration in a work which reported a remaining structural conformation of the molecules in the microarray enough for a successful recognition of epitopes under UV-radiation conditions relevant for Mars [76]. Our results contribute to enlarge the knowledge about the kind of potentially detectable biomarkers on Mars analog sites specifically and in others planetary aims in general.

Taking into account these supportive data and previous studies of the accuracy of a microarray approach for biomolecules detection in environment, a specific MASE-sites microarray was been designed and developed—MASE-Chip—to expand the contribution to the biomarkers detection field.

In the reported MASE-Chip, for the detection and identification of a wide range of biomolecules associated with halophiles and anaerobic, we used polyclonal antibodies. They have some advantages because they are cheaper and faster to produce and because the possibilities for binding any target epitope in a complex sample are theoretically higher than with monoclonal antibodies, especially in a sandwich type assay. The drawback of this selection is the apparently higher cross-reactivity between antigens in the use of polyclonal antibodies. To minimize this handicap, we selected high-titer antibodies, optimized working dilutions in the assays (Table S2), and disentangled cross-reaction occurring in the new array by the transformation of the fluorescence data into a matrix, which was visualized as a heat map and in a graph of nodes and links (Figure 5). Being aware of and taking into account what the heatmap and graph show can help the interpretation of data, in order to discern possible false positives or detection of similar microorganisms or metabolisms. Notwithstanding that in many cases, Abs tested in the microarray recognized more than the one antigen that originated from them (Figure 5), some phylogenetically related and others not, which responded to the mentioned cross-reactivity drawback that happens in multiplexed sandwich assays [77]. The circles and arrows in the graph presented in Figure 5 qualitatively show the events of recognition between Abs in the MASE-chip and their Ag cognates that were used for their performance. An improvement that will

be implemented (and which has proven potential) will be to transform these data into quantitative data [78], which will help us to discard the weakest cross-reactions and keep those relevant.

The MASE-Chip is available to be used in future investigations, both in the field and laboratories in the search for molecular biosignatures. Further studies and improvements will support its accurate applicability for environmental and astrobiology research and, especially due to the nature of the sources used to generate the antibodies that it contains, in anaerobic and salty environments.

Supplementary Materials: The following are available online at <http://www.mdpi.com/2076-2607/7/9/365/s1>, Table S1: List of antibodies printed in the LDChip168 for this study. Table S2: Working dilution and detection limit of Abs in MASE-chip.

Author Contributions: L.G.-D. and F.G.G. planned the study and participated during sampling trips. L.G.-D. performed the experiments and wrote the manuscript. F.G.G. and V.P. supervised and reviewed the manuscript. C.S.C. conceptualized the MASE project as a whole and helped proof reading the manuscript and its revision. A.P., C.M.-E. provided isolates and glacier samples. M.G.-V. helped with experiments. F.W., P.R., K.B.-V., P.E. and R.A. contributed in the results discussion and by proof reading and reviewing the manuscript. P.C. and N.W. gave management support. V.M., P.V., A.R., E.M., M.M., F.G., M.B. and E.R. approved the manuscript after their revision and inputs. Besides, C.S.C., P.R., A.P., C.M.-E., E.M., F.G.G., V.M., P.V., K.B.-V., R.A. and L.G.-D. participated during sampling trips.

Funding: MASE is supported by European Community's Seventh Framework Program (FP7/2007–2013) under Grant Agreement N° 607297.

Acknowledgments: We thank Centro de Astrobiología (CSIC-INTA) for financial/equipment support and Beatriz López Jimenez for her invaluable laboratory assistance.

Conflicts of Interest: The authors declare no conflict of interest.

References

1. Cockell, C.S.; Bush, T.; Bryce, C.; Direito, S.; Fox-Powell, M.; Harrison, J.P.; Lammer, H.; Landenmark, H.; Martin-Torres, J.; Nicholson, N.; et al. Habitability: A Review. *Astrobiology* **2016**, *16*, 89–117. [[CrossRef](#)] [[PubMed](#)]
2. Stoker, C.R.; Zent, A.; Catling, D.C.; Douglas, S.; Marshall, J.R.; Archer, D.; Clark, B.; Kounaves, S.P.; Lemmon, M.T.; Quinn, R.; et al. Habitability of the Phoenix landing site. *J. Geophys. Res.* **2010**, *115*. [[CrossRef](#)]
3. Westall, F.; Loizeau, D.; Foucher, F.; Bost, N.; Bertrand, M.; Vago, J.; Kminek, G. Habitability on Mars from a Microbial Point of View. *Astrobiology* **2013**, *13*, 887–897. [[CrossRef](#)] [[PubMed](#)]
4. Davila, A.F.; Duport, L.G.; Melchiorri, R.; Jäichen, J.; Valea, S.; Rios, A.d.I.; Fairén, A.G.; Möhlmann, D.; McKay, C.P.; Ascaso, C.; et al. Hygroscopic Salts and the Potential for Life on Mars. *Astrobiology* **2010**, *10*, 617–628. [[CrossRef](#)] [[PubMed](#)]
5. Davila, A.F.; Fairén, A.G.; Gago-Duport, L.; Stoker, C.; Amils, R.; Bonaccorsi, R.; Zavaleta, J.; Lim, D.; Schulze-Makuch, D.; McKay, C.P. Subsurface formation of oxidants on Mars and implications for the preservation of organic biosignatures. *Earth Planet. Sci. Lett.* **2008**, *272*, 456–463. [[CrossRef](#)]
6. Fairén, A.G.; Davila, A.F.; Lim, D.; Bramall, N.; Bonaccorsi, R.; Zavaleta, J.; Uceda, E.R.; Stoker, C.; Wierzchos, J.; Dohm, J.M.; et al. Astrobiology through the Ages of Mars: The Study of Terrestrial Analogues to Understand the Habitability of Mars. *Astrobiology* **2010**, *10*, 821–843. [[CrossRef](#)]
7. Horneck, G. The microbial world and the case for Mars. *Planet. Space Sci.* **2000**, *48*, 1053–1063. [[CrossRef](#)]
8. Michalski, J.; Cuadros, J.; Niles, P.; Parnell, J.; Deanne Rogers, A.; Wright, S.P. Groundwater activity on Mars and implications for a deep biosphere. *Nat. Geosci.* **2013**, *6*, 133–138. [[CrossRef](#)]
9. Schulze-Makuch, D.; Irwin, L.N.; Lipps, J.H.; LeMone, D.; Dohm, J.M.; Fairén, A.G. Scenarios for the evolution of life on Mars. *J. Geophys. Res.* **2005**, *110*. [[CrossRef](#)]
10. Tosca, N.J.; Knoll, A.H.; McLennan, S.M. Water Activity and the Challenge for Life on Early Mars. *Science* **2008**, *320*, 1204–1207. [[CrossRef](#)]
11. Gu, W.; Li, Y.; Tang, M.; Jia, X.; Ding, X.; Bi, X.; Wang, X. Water uptake and hygroscopicity of perchlorates and implications for the existence of liquid water in some hyperarid environments. *Rsc. Adv.* **2017**, *7*, 46866–46873. [[CrossRef](#)]

12. Martín-Torres, F.J.; Zorzano, M.-P.; Valentín-Serrano, P.; Harri, A.-M.; Genzer, M.; Kemppinen, O.; Rivera-Valentin, E.G.; Jun, I.; Wray, J.; Bo Madsen, M.; et al. Transient liquid water and water activity at Gale crater on Mars. *Nat. Geosci.* **2015**, *8*, 357. [[CrossRef](#)]
13. McEwen, A.S.; Ojha, L.; Dundas, C.M.; Mattson, S.S.; Byrne, S.; Wray, J.J.; Cull, S.C.; Murchie, S.L.; Thomas, N.; Gulick, V.C. Seasonal Flows on Warm Martian Slopes. *Science* **2011**, *333*, 740. [[CrossRef](#)] [[PubMed](#)]
14. Bibring, J.-P.; Langevin, Y.; Mustard, J.F.; Poulet, F.; Arvidson, R.; Gendrin, A.; Gondet, B.; Mangold, N.; Pinet, P.; Forget, F.; et al. Global Mineralogical and Aqueous Mars History Derived from OMEGA/Mars Express Data. *Science* **2006**, *312*, 400. [[CrossRef](#)] [[PubMed](#)]
15. Carr, M.H.; Head, J.W. Geologic history of Mars. *Earth Planet. Sci. Lett.* **2010**, *294*, 185–203. [[CrossRef](#)]
16. McCauley, J.F. Mariner 9 evidence for wind erosion in the equatorial and mid-latitude regions of Mars. *J. Geophys. Res. (1896–1977)* **1973**, *78*, 4123–4137. [[CrossRef](#)]
17. McEwen, A.S.; Eliason, E.M.; Bergstrom, J.W.; Bridges, N.T.; Hansen, C.J.; Delamere, W.A.; Grant, J.A.; Gulick, V.C.; Herkenhoff, K.E.; Keszthelyi, L.; et al. Mars Reconnaissance Orbiter's High Resolution Imaging Science Experiment (HiRISE). *J. Geophys. Res.* **2007**, *112*. [[CrossRef](#)]
18. Ojha, L.; Wilhelm, M.B.; Murchie, S.L.; McEwen, A.S.; Wray, J.J.; Hanley, J.; Massé, M.; Chojnacki, M. Spectral evidence for hydrated salts in recurring slope lineae on Mars. *Nat. Geosci.* **2015**, *8*, 829. [[CrossRef](#)]
19. Stillman, D.E.; Michaels, T.I.; Grimm, R.E.; Harrison, K.P. New observations of martian southern mid-latitude recurring slope lineae (RSL) imply formation by freshwater subsurface flows. *Icarus* **2014**, *233*, 328–341. [[CrossRef](#)]
20. Bryanskaya, A.; Rozanov, A.; Malup, T.; Aleshina, T.; Lazareva, E.; Taran, O.; Goryachkovskaya, T.; Ivanisenko, V.; Peltek, S. An Integrated Study to Analyze Salt Lake Microbial Community Structure (Novosibirsk Oblast, Russia). *Acta Geol. Sin. Engl. Ed.* **2014**, *88*, 61–62. [[CrossRef](#)]
21. Litchfield, C.D. Survival strategies for microorganisms in hypersaline environments and their relevance to life on early Mars. *Meteorit. Planet. Sci.* **1998**, *33*, 813–819. [[CrossRef](#)]
22. Oren, A.; Elevi Bardavid, R.; Mana, L.J.E. Perchlorate and halophilic prokaryotes: implications for possible halophilic life on Mars. *Extremophiles* **2014**, *18*, 75–80. [[CrossRef](#)] [[PubMed](#)]
23. Leuko, S.; Rothschild, L.J.; Burns, B.P. Halophilic Archaea and the Search for Extinct and Extant Life on Mars. *J. Cosmol.* **2010**, *5*, 940–950.
24. Clark, B.C.; Baird, A.K.; Rose, H.J.; Toulmin, P.; Keil, K.; Castro, A.J.; Kelliher, W.C.; Rowe, C.D.; Evans, P.H. Inorganic Analyses of Martian Surface Samples at the Viking Landing Sites. *Science* **1976**, *194*, 1283–1288. [[CrossRef](#)] [[PubMed](#)]
25. Clark, B.C.; Baird, A.K.; Weldon, R.J.; Tsusaki, D.M.; Schnabel, L.; Candelaria, M.P. Chemical composition of Martian fines. *J. Geophys. Res. Solid Earth* **1982**, *87*, 10059–10067. [[CrossRef](#)]
26. Wänke, H.; Brückner, J.; Dreibus, G.; Rieder, R.; Ryabchikov, I. Chemical Composition of Rocks and Soils at the Pathfinder Site. *Space Sci. Rev.* **2001**, *96*, 317–330. [[CrossRef](#)]
27. Brückner, J.; Dreibus, G.; Rieder, R.; Wänke, H. Refined data of Alpha Proton X-ray Spectrometer analyses of soils and rocks at the Mars Pathfinder site: Implications for surface chemistry. *J. Geophys. Res. Planets* **2003**, *108*. [[CrossRef](#)]
28. Michalski, J.R.; Onstott, T.C.; Mojzsis, S.J.; Mustard, J.; Chan, Q.H.S.; Niles, P.B.; Johnson, S.S. The Martian subsurface as a potential window into the origin of life. *Nat. Geosci.* **2018**, *11*, 21–26. [[CrossRef](#)]
29. Stamenković, V.; Ward, L.M.; Mischna, M.; Fischer, W.W. O₂ solubility in Martian near-surface environments and implications for aerobic life. *Nat. Geosci.* **2018**, *11*, 905–909. [[CrossRef](#)]
30. Cockell, C.S.; Schwendner, P.; Perras, A.; Rettberg, P.; Beblo-Vranesevic, K.; Bohmeier, M.; Rabbow, E.; Moissl-Eichinger, C.; Wink, L.; Marteinsson, V.; et al. Anaerobic microorganisms in astrobiological analogue environments: from field site to culture collection. *Int. J. Astrobiol.* **2018**, *17*, 314–328. [[CrossRef](#)]
31. Perras, A.K. Grappling extremes: Molecular methods combined with cultivation reveal the composition and biology of space-relevant microbial communities. Ph.D. Thesis, University of Regensburg, Regensburg, Germany, 15 January 2018.
32. Beblo-Vranesevic, K.; Bohmeier, M.; Perras, A.K.; Schwendner, P.; Rabbow, E.; Moissl-Eichinger, C.; Cockell, C.S.; Pukall, R.; Vannier, P.; Marteinsson, V.T.; et al. The responses of an anaerobic microorganism, *Yersinia intermedia* MASE-LG-1 to individual and combined simulated Martian stresses. *PLoS ONE* **2017**, *12*, e0185178. [[CrossRef](#)] [[PubMed](#)]

33. Gaboyer, F.; Le Milbeau, C.; Bohmeier, M.; Schwendner, P.; Vannier, P.; Beblo-Vranesevic, K.; Rabbow, E.; Foucher, F.; Gautret, P.; Guégan, R.; et al. Mineralization and Preservation of an extremotolerant Bacterium Isolated from an Early Mars Analog Environment. *Sci. Rep.* **2017**, *7*, 8775. [[CrossRef](#)] [[PubMed](#)]
34. Beblo-Vranesevic, K.; Bohmeier, M.; Perras, A.K.; Schwendner, P.; Rabbow, E.; Moissl-Eichinger, C.; Cockell, C.S.; Vannier, P.; Marteinson, V.T.; Monaghan, E.P.; et al. Lack of correlation of desiccation and radiation tolerance in microorganisms from diverse extreme environments tested under anoxic conditions. *FEMS Microbiol. Lett.* **2018**, *365*, fny044. [[CrossRef](#)] [[PubMed](#)]
35. Schwendner, P.; Bohmeier, M.; Rettberg, P.; Beblo-Vranesevic, K.; Gaboyer, F.; Moissl-Eichinger, C.; Perras, A.K.; Vannier, P.; Marteinson, V.T.; Garcia-Descalzo, L.; et al. Beyond Chloride Brines: Variable Metabolomic Responses in the Anaerobic Organism *Yersinia intermedia* MASE-LG-1 to NaCl and MgSO₄ at Identical Water Activity. *Front. Microbiol.* **2018**, *9*. [[CrossRef](#)] [[PubMed](#)]
36. Parro, V.; Rodríguez-Manfredi, J.A.; Briones, C.; Compostizo, C.; Herrero, P.L.; Vez, E.; Sebastián, E.; Moreno-Paz, M.; García-Villadangos, M.; Fernández-Calvo, P.; et al. Instrument development to search for biomarkers on mars: Terrestrial acidophile, iron-powered chemolithoautotrophic communities as model systems. *Planet. Space Sci.* **2005**, *53*, 729–737. [[CrossRef](#)]
37. Sims, M.R.; Cullen, D.C.; Bannister, N.P.; Grant, W.D.; Henry, O.; Jones, R.; McKnight, D.; Thompson, D.P.; Wilson, P.K. The specific molecular identification of life experiment (SMILE). *Planet. Space Sci.* **2005**, *53*, 781–791. [[CrossRef](#)]
38. Parro, V.; Diego-Castilla, G.d.; Rodríguez-Manfredi, J.A.; Rivas, L.A.; Blanco-López, Y.; Sebastián, E.; Romeral, J.; Compostizo, C.; Herrero, P.L.; García-Marín, A.; et al. SOLID3: A Multiplex Antibody Microarray-Based Optical Sensor Instrument for In Situ Life Detection in Planetary Exploration. *Astrobiology* **2011**, *11*, 15–28. [[CrossRef](#)] [[PubMed](#)]
39. Sephton, M.A.; Sims, M.R.; Court, R.W.; Luong, D.; Cullen, D.C. Searching for biomolecules on Mars: Considerations for operation of a life marker chip instrument. *Planet. Space Sci.* **2013**, *86*, 66–74. [[CrossRef](#)]
40. Parro, V.; Diego-Castilla, G.d.; Moreno-Paz, M.; Blanco, Y.; Cruz-Gil, P.; Rodríguez-Manfredi, J.A.; Fernández-Remolar, D.; Gómez, F.; Gómez, M.J.; Rivas, L.A.; et al. A Microbial Oasis in the Hypersaline Atacama Subsurface Discovered by a Life Detector Chip: Implications for the Search for Life on Mars. *Astrobiology* **2011**, *11*, 969–996. [[CrossRef](#)]
41. Parro, V.; Rivas, L.A.; Gómez-Elvira, J. Protein Microarrays-Based Strategies for Life Detection in Astrobiology. In *Strategies of Life Detection*; Botta, O., Bada, J.L., Gomez-Elvira, J., Javaux, E., Selsis, F., Summons, R., Eds.; Springer: Boston, MA, USA, 2008; Volume 25, pp. 293–311.
42. Blanco, Y.; Gallardo-Carreño, I.; Ruiz-Bermejo, M.; Puente-Sánchez, F.; Cavalcante-Silva, E.; Quesada, A.; Prieto-Ballesteros, O.; Parro Garcia, V. Critical Assessment of Analytical Techniques in the Search for Biomarkers on Mars: A Mummified Microbial Mat from Antarctica as a Best-Case Scenario. *Astrobiology* **2017**, *17*. [[CrossRef](#)]
43. Parro, V.; Blanco, Y.; Puente-Sánchez, F.; Rivas, L.A.; Moreno-Paz, M.; Echeverría, A.; Chong-Díaz, G.; Demergasso, C.; Cabrol Nathalie, A. Biomarkers and Metabolic Patterns in the Sediments of Evolving Glacial Lakes as a Proxy for Planetary Lake Exploration. *Astrobiology* **2018**, *18*, 586–606. [[CrossRef](#)] [[PubMed](#)]
44. Parro, V.; Fernández-Remolar, D.; Rodríguez-Manfredi, J.A.; Cruz-Gil, P.; Rivas, L.A.; Ruiz-Bermejo, M.; Moreno-Paz, M.; García-Villadangos, M.; Gómez-Ortiz, D.; Blanco-López, Y.; et al. Classification of Modern and Old Río Tinto Sedimentary Deposits Through the Biomolecular Record Using a Life Marker Biochip: Implications for Detecting Life on Mars. *Astrobiology* **2011**, *11*, 29–44. [[CrossRef](#)] [[PubMed](#)]
45. Puente-Sánchez, F.; Sánchez-Román, M.; Amils, R.; Parro Garcia, V. *Tessaracoccus lapidicaptus* sp. nov., an actinobacterium isolated from the deep subsurface of the Iberian pyrite belt. *Int. J. Syst. Evol. Microbiol.* **2014**, *64*, 3546–3552. [[CrossRef](#)]
46. Puente-Sánchez, F.; Arce Rodríguez, A.; Oggerin, M.; García-Villadangos, M.; Moreno-Paz, M.; Blanco, Y.; Rodríguez, N.; Bird, L.; Lincoln, S.; Tornos, F.; et al. Viable cyanobacteria in the deep continental subsurface. *Proc. Natl. Acad. Sci. USA* **2018**, *115*. [[CrossRef](#)]
47. Blanco, Y.; Prieto-Ballesteros, O.; Gómez, M.J.; Moreno-Paz, M.; García-Villadangos, M.; Rodríguez-Manfredi, J.A.; Cruz-Gil, P.; Sánchez-Román, M.; Rivas, L.A.; Parro, V. Prokaryotic communities and operating metabolisms in the surface and the permafrost of Deception Island (Antarctica). *Environ. Microbiol.* **2012**, *14*, 2495–2510. [[CrossRef](#)] [[PubMed](#)]

48. Parro, V.; Puente-Sánchez, F.; Cabrol, N.A.; Gallardo-Carreño, I.; Moreno-Paz, M.; Blanco, Y.; García-Villadangos, M.; Tampley, C.; Tilot, V.C.; Thompson, C.; et al. Microbiology and Nitrogen Cycle in the Benthic Sediments of a Glacial Oligotrophic Deep Andean Lake as Analog of Ancient Martian Lake-Beds. *Front. Microbiol.* **2019**, *10*. [[CrossRef](#)]
49. Woods, P.J.E. The geology of Boulby Mine. *Econ. Geol.* **1979**, *74*, 409–418. [[CrossRef](#)]
50. McGenity, T.J.; Gemmell, R.T.; Grant, W.D.; Stan-Lotter, H. Origins of halophilic microorganisms in ancient salt deposits. *Environ. Microbiol.* **2000**, *2*, 243–250. [[CrossRef](#)]
51. Cockell, C.S.; Payler, S.; Paling, S.; McLuckie, D. Boulby International Subsurface Astrobiology Laboratory Boulby Mine. *Astron. Geophys.* **2013**, *54*, 2.25–2.27. [[CrossRef](#)]
52. Payler, S.J.; Biddle, J.F.; Coates, A.J.; Cousins, C.R.; Cross, R.E.; Cullen, D.C.; Downs, M.T.; Direito, S.O.L.; Edwards, T.; Gray, A.L.; et al. Planetary science and exploration in the deep subsurface: Results from the MINAR Program, Boulby Mine, UK. *Int. J. Astrobiol.* **2017**, *16*, 114–129. [[CrossRef](#)]
53. Thorarinsson, S. Grænavatn and Gestsdavvatn. *Geogr. Tidsskr.* **1953**, *52*, 292–302.
54. Bhattacharya, J.P.; Payenberg, T.H.D.; Lang, S.C.; Bourke, M. Dynamic river channels suggest a long-lived Noachian crater lake on Mars. *Geophys. Res. Lett.* **2005**, *32*. [[CrossRef](#)]
55. Ehlmann, B.L.; Mustard, J.F.; Fassett, C.I.; Schon, S.C.; Head Iii, J.W.; Des Marais, D.J.; Grant, J.A.; Murchie, S.L. Clay minerals in delta deposits and organic preservation potential on Mars. *Nat. Geosci.* **2008**, *1*, 355. [[CrossRef](#)]
56. Rudolph, C.; Wanner, G.; Huber, R. Natural Communities of Novel Archaea and Bacteria Growing in Cold Sulfurous Springs with a String-of-Pearls-Like Morphology. *Appl. Environ. Microbiol.* **2001**, *67*, 2336–2344. [[CrossRef](#)] [[PubMed](#)]
57. Henneberger, R.; Moissl, C.; Amann, T.; Rudolph, C.; Huber, R. New insights into the lifestyle of the cold-loving SM1 euryarchaeon: natural growth as a monospecies biofilm in the subsurface. *Appl. Environ. Microbiol.* **2006**, *72*, 192–199. [[CrossRef](#)]
58. Moissl, C.; Rudolph, C.; Huber, R. Natural communities of novel archaea and bacteria with a string-of-pearls-like morphology: molecular analysis of the bacterial partners. *Appl. Environ. Microbiol.* **2002**, *68*, 933–937. [[CrossRef](#)]
59. Lemcke, K. Übertiefe Grundwässer im süddeutschen Alpenvorland. *Buu Ver Schweiz Pet.-Geol U -Ing* **1976**, *42*, 9–18.
60. Probst, A.J.; Birarda, G.; Holman, H.-Y.N.; DeSantis, T.Z.; Wanner, G.; Andersen, G.L.; Perras, A.K.; Meck, S.; Völkel, J.; Bechtel, H.A.; et al. Coupling genetic and chemical microbiome profiling reveals heterogeneity of archaeome and bacteriome in subsurface biofilms that are dominated by the same archaeal species. *PLoS ONE* **2014**, *9*, e99801. [[CrossRef](#)]
61. Gaillard, F.; Michalski, J.; Berger, G.; MacLennan, S.M.; Scaillet, B. Geochemical Reservoirs and Timing of Sulfur Cycling on Mars. *Space Sci. Rev.* **2013**, *174*, 251–300. [[CrossRef](#)]
62. Rivas, L.A.; García-Villadangos, M.; Moreno-Paz, M.; Cruz-Gil, P.; Gómez-Elvira, J.; Parro, V. A 200-Antibody Microarray Biochip for Environmental Monitoring: Searching for Universal Microbial Biomarkers through Immunoprofiling. *Anal. Chem.* **2008**, *80*, 7970–7979. [[CrossRef](#)]
63. Blanco, Y.; Moreno-Paz, M.; Aguirre, J.; Parro, V. Multiplex Fluorescent Antibody Microarrays and Antibody Graphs for Microbial and Biomarker Detection in the Environment. In *Hydrocarbon and Lipid Microbiology Protocol*; McGenity, T.J., Timmis, K.N., Fernandez, B.N., Eds.; Springer: Berlin/Heidelberg, Germany, 2015.
64. Nocker, A.; Sossa-Fernandez, P.; Burr, M.D.; Camper, A.K. Use of propidium monoazide for live/dead distinction in microbial ecology. *Appl. Environ. Microbiol.* **2007**, *73*, 5111–5117. [[CrossRef](#)] [[PubMed](#)]
65. Barth, V.C.; Cattani, F.; Ferreira, C.A.S.; de Oliveira, S.D. Sodium chloride affects propidium monoazide action to distinguish viable cells. *Anal. Biochem.* **2012**, *428*, 108–110. [[CrossRef](#)] [[PubMed](#)]
66. Sánchez-García, L.; Aeppli, C.; Parro, V.; Fernández-Remolar, D.; García-Villadangos, M.; Chong-Díaz, G.; Blanco, Y.; Carrizo, D.J.B. Molecular biomarkers in the subsurface of the Salar Grande (Atacama, Chile) evaporitic deposits. *Biogeochemistry* **2018**, *140*, 31–52. [[CrossRef](#)]
67. Blanco, Y.; Rivas, L.A.; García-Moyano, A.; Aguirre, J.; Cruz-Gil, P.; Palacín, A.; van Heerden, E.; Parro, V. Deciphering the prokaryotic community and metabolisms in South African deep-mine biofilms through antibody microarrays and graph theory. *PLoS ONE* **2014**, *9*, e114180. [[CrossRef](#)] [[PubMed](#)]

68. García-Descalzo, L.; García-López, E.; Alcázar, A.; Baquero, F.; Cid, C. Proteomic analysis of the adaptation to warming in the Antarctic bacteria *Shewanella frigidimarina*. *Biochim. Et Biophys. Acta (Bba) Proteins Proteom.* **2014**, *1844*, 2229–2240. [[CrossRef](#)]
69. Feller, G. Cryosphere and Psychrophiles: Insights into a Cold Origin of Life? *Life (Basel)* **2017**, *7*, 25. [[CrossRef](#)] [[PubMed](#)]
70. Vorobyova, E.; Soina, V.; Gorlenko, M.; Minkovskaya, N.; Zalinova, N.; Mamukelashvili, A.; Gilichinsky, D.; Rivkina, E.; Vishnivetskaya, T. The deep cold biosphere: facts and hypothesis. *Fems Microbiol. Rev.* **1997**, *20*, 277–290. [[CrossRef](#)]
71. Antony, R.; Krishnan, K.P.; Laluraj, C.M.; Thampan, M.; Dhakephalkar, P.K.; Engineer, A.S.; Shivaji, S. Diversity and physiology of culturable bacteria associated with a coastal Antarctic ice core. *Microbiol. Res.* **2012**, *167*, 372–380. [[CrossRef](#)] [[PubMed](#)]
72. Marx, J.G.; Carpenter, S.D.; Deming, J.W. Production of cryoprotectant extracellular polysaccharide substances (EPS) by the marine psychrophilic bacterium *Colwellia psychrerythraea* strain 34H under extreme conditions. *Can. J. Microbiology.* **2009**, *55*, 63–72. [[CrossRef](#)]
73. Cousins, C. Volcanogenic Fluvial-Lacustrine Environments in Iceland and Their Utility for Identifying Past Habitability on Mars. *Life (Basel)* **2015**, *5*, 568–586. [[CrossRef](#)]
74. Johnston, C.A. Sediment and nutrient retention by freshwater wetlands: Effects on surface water quality. *Crit. Rev. Environ. Control* **1991**, *21*, 491–565. [[CrossRef](#)]
75. Knox, A.K.; Dahlgren, R.A.; Tate, K.W.; Atwill, E.R. Efficacy of Natural Wetlands to Retain Nutrient, Sediment and Microbial Pollutants. *J. Environ. Qual.* **2008**, *37*, 1837–1846. [[CrossRef](#)] [[PubMed](#)]
76. Blanco, Y.; de Diego-Castilla, G.; Viúdez-Moreiras, D.; Cavalcante-Silva, E.; Rodríguez-Manfredi, J.A.; Davila, A.F.; McKay, C.P.; Parro, V. Effects of Gamma and Electron Radiation on the Structural Integrity of Organic Molecules and Macromolecular Biomarkers Measured by Microarray Immunoassays and Their Astrobiological Implications. *Astrobiology* **2018**, *18*, 1497–1516. [[CrossRef](#)] [[PubMed](#)]
77. Juncker, D.; Bergeron, S.; Laforte, V.; Li, H. Cross-reactivity in antibody microarrays and multiplexed sandwich assays: shedding light on the dark side of multiplexing. *Curr. Opin. Chem. Biol.* **2014**, *18*, 29–37. [[CrossRef](#)] [[PubMed](#)]
78. Rivas, L.A.; Aguirre, J.; Blanco, Y.; González-Toril, E.; Parro, V. Graph-based deconvolution analysis of multiplex sandwich microarray immunoassays: applications for environmental monitoring. *Environ. Microbiol.* **2011**, *13*, 1421–1432. [[CrossRef](#)] [[PubMed](#)]



© 2019 by the authors. Licensee MDPI, Basel, Switzerland. This article is an open access article distributed under the terms and conditions of the Creative Commons Attribution (CC BY) license (<http://creativecommons.org/licenses/by/4.0/>).